*A project report on*

# Finite Element Simulation of Pulsatile Non-Newtonian Blood Flow in Idealized Aneurysmal Geometries

*Submitted in partial fulfillment for the award of the degree of*

## Bachelor of Technology in Computer Science and Engineering

*by*

**Syed Khalid (21BEE1288)**

**Pankaj Kumar (21BCE1655)**

**Aravind Srinivasan (21BCE1733)**


VIT®

Vellore Institute of Technology

(Deemed to be University under section 3 of UGC Act, 1956)

CHENNAI

**April, 2025**

*A project report on*

# Finite Element Simulation of Pulsatile Non-Newtonian Blood Flow in Idealized Aneurysmal Geometries

*Submitted in partial fulfillment for the award of the degree of*

## Bachelor of Technology in Computer Science and Engineering

*by*

**Syed Khalid (21BEE1288)**

**Pankaj Kumar (21BCE1655)**

**Aravind Srinivasan (21BCE1733)**


VIT®

Vellore Institute of Technology

(Deemed to be University under section 3 of UGC Act, 1956)

CHENNAI

**April, 2025**

VIT®
Vellore Institute of Technology
(Deemed to be University under section 3 of UGC Act, 1956)
CHENNAI

## School of Computer Science and Engineering

# CERTIFICATE

This is to certify that the report entitled "**FINITE ELEMENT SIMULATION OF PULSATILE NON-NEWTONIAN BLOOD FLOW IN IDEALIZED ANEURYSMAL GEOMETRIES WITH STENTING STRATEGIES**" is prepared and submitted by **Pankaj Kumar (21BCE1655)** to Vellore Institute of Technology, Chennai, in partial fulfillment of the requirement for the award of the degree of **Bachelor of Technology in Computer Science and Engineering** is a bonafide record carried out under my guidance. The project fulfills the requirements as per the regulations of this University and in my opinion meets the necessary standards for submission. The contents of this report have not been submitted and will not be submitted either in part or in full, for the award of any other degree or diploma and the same is certified.

Signature of the Guide:
Name: Dr. Asha Jerlin
Date:

**Signature of the Examiner**
Name:
Date:

**Signature of the Examiner**
Name:
Date:

**Approved by the Head of Department,**
CSE Core
Name: **Nithyanandam P**
Date: 09-04-2025

# ABSTRACT

The simulation of blood flow in aneurysmal arteries, particularly under non-Newtonian and pulsatile conditions, is of considerable importance in biomedical engineering. This project explores a computational framework using the Finite Element Method (FEM) to simulate such flows through an idealized aneurysm geometry, both pre- and post-stenting. Blood is modeled as a shear-thinning fluid via the power-law formulation, with pulsatile inflow captured using a Crank–Nicolson time integration scheme. The simulation compares two common stent designs — coil embolization and flow-diverting stents — for their impact on hemodynamic parameters.

# ACKNOWLEDGEMENT

I express my heartfelt thanks to my guide **Dr. Asha Jerlin**, SCOPE, VIT Chennai, for her tireless guidance and insight. My sincere gratitude extends to the academic leadership, HoD, and faculty of VIT for their continued support. I also thank my friends and family for their encouragement throughout the project.

**Place:** Chennai
**Date:** **Pankaj Kumar**

# Contents

# List of Figures

# List of Tables

# LIST OF ACRONYMS

| **Acronym** | **Definition** |
|---|---|
| FEM | Finite Element Method |
| CFD | Computational Fluid Dynamics |
| WSS | Wall Shear Stress |
| OSI | Oscillatory Shear Index |
| MUMPS | MUltifrontal Massively Parallel Sparse Solver |
| CN | Crank–Nicolson |

# 1 INTRODUCTION

## 1.1 Background

Aneurysms are pathological dilations in blood vessels that occur due to structural weakness in the vascular wall. These abnormalities, while potentially asymptomatic, can result in life-threatening hemorrhages if ruptured. Their prevalence in cerebral arteries makes them especially dangerous, given the complexity of brain perfusion and the risks associated with neurosurgical intervention.

The blood flow through such regions is governed by several intricate factors: the geometry of the vessel, the pulsatile nature of cardiac output, and the rheological properties of blood. While historically modeled as a Newtonian fluid, blood is in fact a complex suspension of plasma, red blood cells, white cells, and platelets. At low shear rates—such as those present near aneurysmal walls—it exhibits higher viscosity due to erythrocyte aggregation. At higher shear rates, the cells align and deform, leading to reduced viscosity. This non-linear behavior demands a non-Newtonian rheological model to realistically simulate flow.

To further complicate matters, blood is not pumped at a constant rate. The cardiac cycle introduces periodic fluctuations in velocity and pressure, referred to as pulsatile flow. These pulsations cause changes in wall shear stress (WSS), which play a critical role in the initiation and progression of aneurysms. Any comprehensive simulation must therefore be time-dependent and use a constitutive equation that adapts to local shear conditions.

Computational modeling through the Finite Element Method (FEM) has become a central tool in studying such problems. With its ability to handle irregular geometries and solve coupled nonlinear PDEs, FEM is particularly suited for simulating blood flow in biologically realistic domains. In this project, FEATool Multiphysics is used as the simulation platform to model flow through an idealized 3D aneurysmal artery, both in untreated and

stented configurations.

## 1.2 Significance of the Study

Accurate simulation of flow in aneurysmal regions has several biomedical implications. From a clinical standpoint, understanding the hemodynamic environment can aid in identifying aneurysms at high risk of rupture. Surgeons can benefit from predictive models that simulate how stents and coils modify flow, enabling better treatment planning.

From a computational perspective, this study emphasizes the necessity of abandoning simplistic models in favor of physiologically accurate ones. Non-Newtonian rheology and time-dependence are no longer optional—they are essential features for any credible simulation. Furthermore, numerical solvers such as MUMPS and temporal discretization schemes like Crank–Nicolson ensure that our approach remains stable and accurate even under pulsatile conditions.

Finally, this project also serves as a pedagogical case study for how to build FEM simulations from first principles. Everything from geometry creation, meshing, PDE specification, to boundary condition tuning is explored in a structured way. This has value both for researchers entering the field and for students seeking to understand applied mathematics in the biomedical context.

## 1.3 Purpose and Objectives

This capstone project aims to construct a detailed FEM-based simulation of pulsatile, non-Newtonian flow in aneurysmal arteries. The simulation compares pre- and post-treatment states for two stent modalities:

- **Coil embolization**, which effectively occludes the aneurysm.
- **Flow-diverting stents**, which redirect flow past the bulge while preserving downstream perfusion.

The overall goals of the study are:

1. To construct an idealized 3D aneurysm geometry and define a high-quality FEM mesh.
2. To implement the power-law model for shear-dependent viscosity of blood.
3. To apply a physiologically realistic pulsatile velocity waveform at the inlet.
4. To compare velocity profiles, vortex structure, and wall shear stress in treated vs. untreated models.
5. To assess the stability and computational performance of the simulation using MUMPS and Crank–Nicolson.

Although the computational work remains theoretical due to hardware limitations, the full framework is designed to be modular and extensible to patient-specific datasets in future work.

## 1.4 Structure of the Report

This report is organized into several chapters to reflect both the theoretical development and the practical considerations of the simulation:

- **Chapter 2: Literature Review** surveys relevant work in aneurysm modeling, non-Newtonian flow, and numerical simulation.
- **Chapter 3: Problem Statement and Objectives** formalizes the research questions and project goals.
- **Chapter 4: Finite Element Method Theory** details the mathematical framework, including weak formulations and numerical solvers.
- **Chapter 5: Non-Newtonian Fluid Mechanics** introduces the rheological models, focusing on power-law and viscoelastic behavior.
- **Chapter 6: Aneurysm Modeling and Pulsatile Flow** discusses the anatomy, flow physiology, and stenting strategies in aneurysmal treatment.
- **Chapter 7: Simulation Setup and Methodology** outlines the software tools, geometry construction, boundary conditions, and solver settings.

- **Chapter 8: Results and Analysis** presents the key outcomes from simulated models, including comparisons between stented and unstented geometries.
- **Chapter 9: Conclusion and Future Work** summarizes insights and suggests directions for extending the study into real-world applications.

Together, these chapters present a rigorous theoretical framework and simulation-ready workflow for modeling viscoelastic blood flow in aneurysmal vessels.

# 2 LITERATURE REVIEW

Over the last few decades, the simulation of blood flow through arterial systems has evolved significantly, particularly in the context of aneurysmal modeling and endovascular treatment planning. Numerical methods such as Computational Fluid Dynamics (CFD) and Finite Element Method (FEM) have been widely adopted for their ability to resolve complex geometries and flow regimes. This chapter surveys key contributions in the fields of viscoelastic flow modeling, rheological constitutive equations, and computational stent deployment, with a particular focus on how our current work advances beyond existing literature.

## 2.1 Modeling of Viscoelastic and Non-Newtonian Flow

One of the foundational contributions to the theory of viscoelastic fluids is due to Oldroyd [1], who formulated a generalized class of rheological equations still used today. These models—particularly the Oldroyd-B model—incorporate both elastic and viscous stresses, capturing the dual behavior exhibited by biological fluids such as blood. Owens and Phillips [**?**] expanded this framework through a computational lens, providing numerical techniques for solving constitutive models under flow.

More recently, Baaijens [2] reviewed mixed FEM approaches for viscoelastic flow analysis, highlighting the importance of numerical stability and accuracy in non-Newtonian contexts. While much of this work has been developed for benchmark fluid problems, its application to biomedical domains, particularly in three dimensions, has remained relatively sparse.

Varchanis et al. [3] proposed an FEM formulation that circumvents both the Ladyzhenskaya–Babuška–Brezzi (LBB) condition and the high-Weissevnberg number problem—two classical hurdles in viscoelastic simulations. Their methodology, though mathematically

rigorous, was not applied to physiologically relevant geometries such as cerebral aneurysms.

Despite these advances, a research gap persists: **most simulations of aneurysmal blood flow simplify the fluid as Newtonian**, which fails to capture key phenomena like shear-thinning and elasticity. Additionally, many existing studies are limited to **2D planar or axisymmetric models**, neglecting the full spatial complexity of aneurysm morphology.

## 2.2 CFD and FEM Applications in Stenting

The implementation of CFD to analyze stent behavior has been widely reported, particularly for coronary arteries. In the study *Computational Fluid Dynamics Study of Common Stent Models Inside Idealised Curved Coronary Arteries*, the authors analyzed the influence of different stent designs on flow disturbances and wall shear stress. However, their simulations largely assumed Newtonian behavior and lacked time-dependent inlet conditions.

Similarly, in the work on *CFD and FEM of a Customized Stent-Graft for EVAR Treatment of Abdominal Aortic Aneurysm*, a stent-graft was modeled within a patient-specific geometry. The approach demonstrated the utility of simulation in treatment planning, but again assumed steady-state conditions and Newtonian rheology.

While these studies contribute meaningfully to our understanding of device–flow interactions, they stop short of incorporating:

- Non-Newtonian, viscoelastic models for blood,
- Fully 3D, anatomically flexible aneurysm geometries,
- Pulsatile inflow conditions over the cardiac cycle,
- Comparative analysis of multiple stenting modalities within a unified framework.

Our work seeks to bridge this gap by offering a high-fidelity simulation of blood flow through an idealized 3D aneurysm, using power-law fluid models and pulsatile boundary conditions. In addition, we examine the effects of two distinct stenting strategies—coil embolization and flow-diverting mesh—within a consistent numerical framework.

## 2.3 Summary of Research Gap

From the literature reviewed, three key limitations are evident in the current state-of-the-art:

1. **Underutilization of Non-Newtonian Models:** Despite overwhelming physiological evidence, many studies default to Newtonian assumptions for simplicity.
2. **Lack of Pulsatile Boundary Conditions:** Time-dependence is often ignored, even though it profoundly affects WSS and vortex dynamics.
3. **Dimensional Simplification:** Numerous studies restrict themselves to 2D or simplified 3D geometries

# 3 PROBLEM STATEMENT AND OBJECTIVES

## 3.1 Problem Statement

Cardiovascular diseases remain a leading cause of global mortality, with cerebral aneurysms posing particularly grave risks due to their often-silent progression and catastrophic rupture potential. These pathologies involve complex fluid–structure interactions within the vasculature, governed by pulsatile, three-dimensional, and non-Newtonian flow fields. Despite advancements in computational modeling, a gap remains in the literature concerning simulations that fully embrace the physiological intricacies of aneurysmal blood flow—particularly when accounting for non-Newtonian rheology, pulsatile inlet conditions, and realistic stent geometries.

Traditional models often simplify the fluid as Newtonian and the geometry as axisymmetric or two-dimensional. While this reduces computational overhead, it also suppresses critical flow characteristics such as localized recirculation, three-dimensional vortex shedding, and oscillatory wall shear stress (WSS). These phenomena have been repeatedly implicated in aneurysm progression, thrombus formation, and rupture risk.

Moreover, a lack of standardization exists in how stents are modeled computationally. Some studies use overly simplified porous boundaries, while others omit stent modeling entirely. There is little consensus on how different stent types—particularly coil embolization versus flow-diverting meshes—compare in terms of altering intra-aneurysmal flow.

Given this background, there is a compelling need to develop a computational framework that:

- Models blood as a shear-thinning, non-Newtonian fluid,

- Incorporates fully transient, pulsatile boundary conditions,
- Resolves three-dimensional flow domains with aneurysmal bulging,
- Includes comparative analysis of different stent modalities under identical flow conditions.

This project addresses these needs by building a finite element simulation pipeline using FEATool Multiphysics. It is designed to simulate pulsatile, non-Newtonian flow in both stented and unstented aneurysms with attention to physiological realism and numerical rigor.

## 3.2 Detailed Objectives

The aim of this project is to construct a 3D finite element simulation environment for modeling pulsatile blood flow in cerebral aneurysms, with particular focus on comparing stented and unstented conditions under non-Newtonian flow assumptions.

To accomplish this, the project is subdivided into the following structured objectives:

### 3.2.1 Objective 1: Construct a Physiologically Representative Geometry

The first step involves creating an idealized aneurysm geometry using built-in primitives in FEATool. The geometry is designed to replicate the common fusiform or saccular shape observed in cerebral arteries, connected to a cylindrical vessel. Care is taken to ensure smooth curvature and no artificial flow discontinuities.

### 3.2.2 Objective 2: Generate an Appropriate Finite Element Mesh

A high-quality tetrahedral mesh must be generated, with localized mesh refinement near the aneurysm neck and walls to resolve boundary layer gradients. Mesh quality metrics—such as skewness, aspect ratio, and element size distribution—are assessed to ensure numerical stability.

### 3.2.3 Objective 3: Implement Non-Newtonian Power-Law Rheology

Blood is modeled using the power-law formulation, with the viscosity $\mu$ as a function of shear rate $\dot{\gamma}$:

$$\mu = K\dot{\gamma}^{n-1}$$

where $K$ is the consistency index and $n$ is the flow behavior index. For shear-thinning fluids like blood, $n < 1$.

### 3.2.4 Objective 4: Apply Time-Dependent, Pulsatile Boundary Conditions

A physiological waveform is defined at the inlet, mimicking one cardiac cycle. This time-dependent velocity boundary condition is interpolated across simulation steps using Crank–Nicolson time integration to balance stability and accuracy. Outlet conditions are set to allow pressure recovery without artificial reflections.

### 3.2.5 Objective 5: Model Two Stent Modalities

Two common stent implementations are considered:

- **Coil Embolization:** The aneurysmal bulge is treated as a solid domain, simulating near-total occlusion.
- **Flow-Diverting Stent:** A porous shell or resistance boundary is applied along the vessel wall near the aneurysm neck, redirecting blood flow past the bulge.

Each model is implemented as a separate simulation case within the same geometric framework.

### 3.2.6 Objective 6: Solve Using FEM with Advanced Solver Options

The simulations are solved using the MUMPS sparse matrix solver, known for its efficiency with large, sparse systems. Time discretization is handled using the Crank–Nicolson method, which is unconditionally stable for linear problems and moderately stiff nonlinear systems.

### 3.2.7 Objective 7: Visualize and Interpret Hemodynamic Parameters

Key flow characteristics such as:

- Wall Shear Stress (WSS),
- Velocity streamlines,
- Recirculation zones,
- Vorticity and pressure gradients,

are extracted from each simulation and used to compare stented vs. unstented outcomes.

### 3.2.8 Objective 8: Define a Framework for Future Extension

Though the current study uses idealized geometry and artificial inlet profiles, the simulation framework is built to be extendable to:

- Patient-specific geometries from DICOM/CT data,
- Advanced rheological models such as Casson or Carreau-Yasuda,
- Fluid–structure interaction (FSI) with vessel wall elasticity,
- Machine learning surrogate models for faster prediction of flow outcomes.

By rigorously defining each stage of the simulation—from geometry to solver to analysis—this project establishes a modular and reproducible workflow for advanced hemodynamic modeling in cerebrovascular research.

# 4 FINITE ELEMENT METHOD THEORY

## 4.1 Introduction to FEM in Biofluid Context

The Finite Element Method (FEM) [1] is a numerical technique tailored to solving complex partial differential equations (PDEs) over irregular geometries and under varied boundary conditions. Its adaptability, modular structure, and mathematical rigor have made it a dominant method in engineering simulations, especially in fields where spatially varying parameters and nonlinear constitutive models are the norm [4]. In biofluid mechanics — and particularly in aneurysm modeling — FEM offers unmatched flexibility in discretizing tortuous anatomical domains, resolving sharp pressure gradients, and coupling multiple physics such as non-Newtonian rheology and pulsatile flow behavior.

In the context of this project, FEM serves as the computational backbone for simulating transient, incompressible, non-Newtonian blood flow through an aneurysmal artery[4]. Unlike classical CFD approaches that use the Finite Volume or Finite Difference methods, FEM proceeds via the weak (variational) form of the governing equations [2]. This approach naturally incorporates boundary conditions, accommodates irregular meshes, and reduces regularity requirements on the solution.

Blood flow through aneurysms is influenced by a range of spatial and temporal complexities — localized flow recirculation, wall shear stress oscillations, secondary flow patterns, and dynamic pressure loading. Accurately capturing these features requires a numerical framework that can resolve fine geometric details and incorporate time-dependent, non-linear fluid behavior. FEM enables this by discretizing the computational domain into small subregions (elements) and approximating the governing PDEs within each element using localized interpolation (shape) functions.

This chapter develops the theoretical foundation of FEM as applied to our case[5]. It begins with the governing equations of motion in their strong form, derives the

weak formulation step-by-step, and builds toward full discretization and numerical solution strategies using MUMPS and Crank–Nicolson schemes.

## 4.2 Governing Equations: Strong Form

The motion of an incompressible, non-Newtonian fluid is governed by the time-dependent Navier–Stokes equations, which express conservation of momentum and mass[6]:

**Momentum conservation:**

$$\rho\left(\frac{\partial \mathbf{u}}{\partial t} + \mathbf{u}\cdot\nabla\mathbf{u}\right) = -\nabla p + \nabla\cdot\boldsymbol{\tau} + \mathbf{f} \tag{4.1}$$

**Continuity (incompressibility):**

$$\nabla\cdot\mathbf{u} = 0 \tag{4.2}$$

Here, $\mathbf{u}(\mathbf{x},t)$ is the velocity field, $p(\mathbf{x},t)$ is the pressure, $\rho$ is the fluid density, and $\mathbf{f}$ is a body force vector (e.g., gravity). The deviatoric stress tensor $\boldsymbol{\tau}$ represents internal viscous stresses.

For Newtonian fluids, $\boldsymbol{\tau} = \mu(\nabla\mathbf{u} + \nabla\mathbf{u}^T)$ with constant $\mu$. However, in this study we assume a power-law rheology for blood:

$$\mu(\dot\gamma) = K\dot\gamma^{n-1}, \quad \dot\gamma = \sqrt{2\mathbf{D}:\mathbf{D}}, \quad \mathbf{D} = \frac{1}{2}(\nabla\mathbf{u} + \nabla\mathbf{u}^T)$$

This captures the shear-thinning behavior of blood, where viscosity decreases with increasing shear rate $\dot\gamma$. The flow behavior index $n < 1$ and consistency index $K$ are material-specific.

These equations, posed over a 3D domain with suitable initial and boundary conditions, constitute the strong form. However, solving them directly is analytically intractable, particularly over complex geometries like aneurysmal vessels. We therefore turn to the variational (weak) form.

## 4.3 Derivation of the Weak Form

To derive the weak form, we begin by multiplying the strong form of the momentum equation by a suitable test function $\mathbf{v} \in \mathbf{V}$, where $\mathbf{V}$ is a function space of sufficiently smooth, divergence-free vector fields that vanish on Dirichlet boundaries. Integrating over the domain $\Omega$, we obtain:

$$\int_\Omega \rho \left( \frac{\partial \mathbf{u}}{\partial t} + \mathbf{u} \cdot \nabla \mathbf{u} \right) \cdot \mathbf{v} \, d\Omega = - \int_\Omega \nabla p \cdot \mathbf{v} \, d\Omega + \int_\Omega \nabla \cdot \boldsymbol{\tau} \cdot \mathbf{v} \, d\Omega + \int_\Omega \mathbf{f} \cdot \mathbf{v} \, d\Omega \quad (4.3)$$

Using the identity:

$$\int_\Omega \nabla \cdot \boldsymbol{\tau} \cdot \mathbf{v} \, d\Omega = - \int_\Omega \boldsymbol{\tau} : \nabla \mathbf{v} \, d\Omega + \int_{\partial\Omega} (\boldsymbol{\tau} \cdot \mathbf{n}) \cdot \mathbf{v} \, dS$$

and applying integration by parts to the pressure term:

$$- \int_\Omega \nabla p \cdot \mathbf{v} \, d\Omega = \int_\Omega p \nabla \cdot \mathbf{v} \, d\Omega - \int_{\partial\Omega} p \mathbf{n} \cdot \mathbf{v} \, dS$$

Substituting these into the weak form gives:

$$\begin{aligned} \int_\Omega \rho \left( \frac{\partial \mathbf{u}}{\partial t} + \mathbf{u} \cdot \nabla \mathbf{u} \right) \cdot \mathbf{v} \, d\Omega + \int_\Omega \boldsymbol{\tau} : \nabla \mathbf{v} \, d\Omega - \int_\Omega p \nabla \cdot \mathbf{v} \, d\Omega \\ = \int_\Omega \mathbf{f} \cdot \mathbf{v} \, d\Omega + \int_{\partial\Omega} [(\boldsymbol{\tau} - p\mathbf{I}) \cdot \mathbf{n}] \cdot \mathbf{v} \, dS \end{aligned} \quad (4.4)$$

The boundary integral term represents natural (Neumann) boundary conditions, often modeling traction forces or outlet pressures. For example, setting this term to zero implies a traction-free boundary. On Dirichlet boundaries (inflow walls), $\mathbf{v}$ vanishes, eliminating these terms.

The continuity equation is imposed weakly by introducing a scalar test function $q \in Q$ from the pressure function space:

$$\int_\Omega q \nabla \cdot \mathbf{u} \, d\Omega = 0 \quad \forall q \in Q$$

The final weak formulation becomes:

**Find** $\mathbf{u} \in \mathbf{V},\ p \in Q$ **such that for all** $\mathbf{v} \in \mathbf{V},\ q \in Q$:

$$\int_\Omega \rho \left( \frac{\partial \mathbf{u}}{\partial t} + \mathbf{u} \cdot \nabla \mathbf{u} \right) \cdot \mathbf{v}\, d\Omega + \int_\Omega \mu(\dot{\gamma}) \nabla \mathbf{u} : \nabla \mathbf{v}\, d\Omega - \int_\Omega p \nabla \cdot \mathbf{v}\, d\Omega + \int_\Omega q \nabla \cdot \mathbf{u}\, d\Omega = \int_\Omega \mathbf{f} \cdot \mathbf{v}\, d\Omega \tag{4.5}$$

This variational form is now suitable for discretization using finite element spaces. It incorporates both essential and natural boundary conditions directly, handles nonlinear viscosity through $\mu(\dot{\gamma})$, and allows time-dependent evolution.

## 4.4 Element Interpolation and Shape Functions

In the finite element method, the continuous problem is discretized by approximating field variables using basis functions defined over individual elements. These basis (or shape) functions interpolate the values of unknowns (e.g., velocity and pressure) between nodes. The choice of element type and interpolation order has profound effects on both numerical accuracy and computational efficiency.

In three-dimensional domains such as the one under study, tetrahedral elements are frequently employed due to their geometric flexibility and ability to conform to complex vascular structures. Each tetrahedron is defined by four nodes (linear interpolation) or more (quadratic, cubic). Within each element, the velocity field $\mathbf{u}_h$ and pressure field $p_h$ are expressed as:

$$\mathbf{u}_h(\mathbf{x}) = \sum_{i=1}^{N_u} \mathbf{u}_i \phi_i(\mathbf{x}), \quad p_h(\mathbf{x}) = \sum_{j=1}^{N_p} p_j \psi_j(\mathbf{x})$$

where $\phi_i$ and $\psi_j$ are the velocity and pressure shape functions, respectively. These functions are typically chosen from the Lagrange family and satisfy the Kronecker delta property: $\phi_i(\mathbf{x}_j) = \delta_{ij}$.

The proper pairing of function spaces for velocity and pressure is critical for satisfying the Ladyzhenskaya–Babuška–Brezzi (LBB) condition, which ensures the stability of saddle-point problems like incompressible flow.

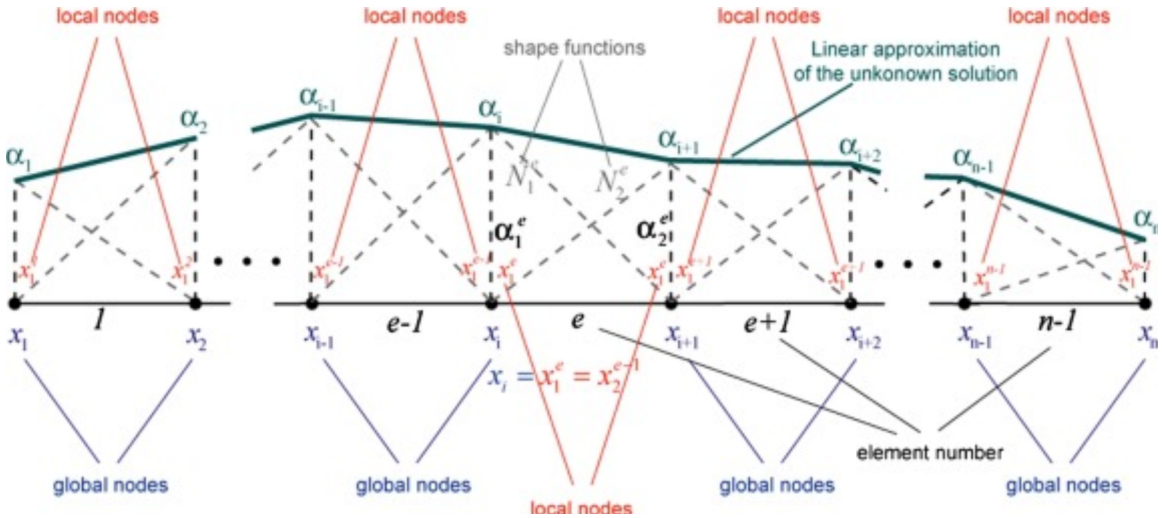


Figure 4.1: Basis functions interpolated over nodes

## 4.5 Assembly of the Global System

Once the weak form is discretized over each element, the local element matrices must be assembled into a global linear system. This process involves iterating over each finite element in the mesh, computing local stiffness, mass, and force contributions, and placing them into the corresponding locations in global matrices.

The result is a system of equations of the form:

$$\mathbf{M}\frac{d\mathbf{U}}{dt} + \mathbf{K}(\mathbf{U})\mathbf{U} + \mathbf{G}P = \mathbf{F} \tag{4.6}$$

$$\mathbf{D}\mathbf{U} = 0 \tag{4.7}$$

Here, $\mathbf{M}$ is the global mass matrix, $\mathbf{K}$ is the nonlinear stiffness matrix (which includes contributions from viscosity and convective terms), $\mathbf{G}$ and $\mathbf{D}$ represent gradient and divergence operators coupling velocity and pressure, and $\mathbf{F}$ is the external force vector.

Due to the sparsity and size of these matrices — especially in 3D — efficient assembly and storage schemes are employed. Most entries are zero, and only nonzero values are stored and processed.

## 4.6 Time Integration: Crank–Nicolson Method

To evolve the velocity field in time, a Crank–Nicolson scheme is used, which offers second-order temporal accuracy while maintaining stability in stiff systems. Applied to the momentum equation, it takes the form:

$$\frac{\mathbf{M}(\mathbf{U}^{n+1} - \mathbf{U}^n)}{\Delta t} = \frac{1}{2}\left[\mathbf{F}(\mathbf{U}^{n+1}) + \mathbf{F}(\mathbf{U}^n)\right]$$

where $\mathbf{F}(\mathbf{U})$ encapsulates all right-hand side contributions including convective, viscous, and pressure terms. This formulation requires solving a nonlinear system at each time step, often using fixed-point iteration or Newton–Raphson methods for convergence.

The Crank–Nicolson method balances the numerical damping of fully implicit schemes with the temporal accuracy of explicit methods — making it well-suited for capturing pulsatile flow where temporal gradients are significant.

## 4.7 Boundary Conditions in Biomedical Flow Modeling

Boundary conditions (BCs) in FEM simulations govern how the model interacts with its surroundings. In the present simulation, different types of BCs are applied based on the physiological region and clinical objective:

On the inflow boundary (proximal artery), a time-dependent Dirichlet condition is imposed to represent the cardiac cycle's pulsatile velocity waveform. This condition varies sinusoidally or using patient-specific profiles derived from Doppler or MRI measurements.

At the outflow boundary (distal artery), a pressure condition is applied — often zero-gauge or a constant pressure drop — modeled either as a natural Neumann condition or as part of a resistance boundary model.

The vessel wall is modeled as a no-slip Dirichlet condition: $\mathbf{u} = 0$. This assumption, though simplistic, is common in blood flow modeling where wall motion is not the primary focus.

For stented regions: - A **coil-embolized aneurysm** is treated as an internal wall — effectively a domain exclusion or no-flow boundary. - A **flow-diverter stent** is

modeled as a resistive surface, either via Robin-type boundary conditions or porous interface approximations.

The choice of BCs directly influences the flow field, especially recirculation patterns, wall shear stress distributions, and vortex persistence in the aneurysm dome.

## 4.8 Solver: MUltifrontal Massively Parallel Sparse Solver (MUMPS)

Given the large, sparse, nonlinear systems arising from FEM discretization, an efficient linear solver is critical. MUMPS is a state-of-the-art sparse direct solver that decomposes the global system using a multifrontal LU factorization strategy. It is especially adept at handling the symmetric but indefinite matrices that arise in saddle-point formulations.

Key advantages of MUMPS include: - Robust performance on sparse systems from 3D PDEs, - Support for parallel computing environments (MPI), - Compatibility with mixed-element meshes and complex domains.

Its use in this project ensures that simulations remain stable and converge within acceptable computational time, even with several hundred thousand degrees of freedom.

## 4.9 Implementation in FEATool Multiphysics

FEATool Multiphysics serves as the simulation environment for this project. Its modular architecture allows: - Geometry creation using built-in primitives, - Mesh generation with element quality control, - PDE definition using weak form syntax and GUI or script interface, - Solver configuration including Crank–Nicolson and MUMPS backends, - Postprocessing with contour plots, streamline visualization, and point probes.

The modeling workflow progresses from geometry definition to boundary condition setup, PDE coefficient assignment, meshing, and simulation run. Separate models are prepared for the unstented, coil-stented, and mesh-stented cases — enabling direct comparison of hemodynamic metrics such as velocity magnitude, wall shear stress, and vortex structures.

# 5 NON-NEWTONIAN AND VISCOELASTIC FLUID MECHANICS

## 5.1 Introduction to Non-Newtonian Fluid Behavior

In classical fluid dynamics, Newtonian fluids are characterized by a constant viscosity independent of shear rate. Water, air, and simple oils follow this assumption. However, in biological contexts — particularly with blood — this simplification fails to capture essential physiological behavior [7].

Blood is a complex suspension of plasma, red blood cells (RBCs), white blood cells, and platelets. Its rheology is shear-dependent: under low shear conditions (e.g., in aneurysms or capillaries), blood behaves as a viscous gel due to RBC aggregation. At high shear rates, these aggregates disassociate, and the viscosity decreases. This phenomenon is known as shear-thinning and places blood firmly in the category of non-Newtonian fluids.

In addition to shear-dependence, blood exhibits viscoelastic properties, combining both fluidic flow and elastic memory effects. These are particularly relevant in pulsatile flows, where deformation history influences current stress states — a behavior unaccounted for in Newtonian formulations[3].

## 5.2 Power-Law Fluids: Shear-Thinning and Thixotropy

One of the most widely used models for capturing shear-dependent viscosity is the power-law model [8]. This model assumes the apparent viscosity $\mu$ varies with shear rate $\dot{\gamma}$ as:

$$\mu(\dot{\gamma}) = K\dot{\gamma}^{n-1}$$

Here, $K$ is the consistency index and $n$ is the flow behavior index. When $n < 1$, the fluid exhibits shear-thinning behavior; for $n > 1$, it becomes shear-thickening.

In the context of blood: - Typical values are $n \approx 0.6$–$0.9$, depending on hematocrit and flow conditions. - The model does not account for yield stress, but within cerebral arteries and aneurysms, this is often acceptable. - It offers computational simplicity while still capturing the nonlinearity of real blood flow, especially near the vessel walls.

While the power-law model is not strictly accurate at zero or very high shear rates, it provides a good approximation within the physiological range encountered in aneurysms.

## 5.3 Viscoelastic Models: Oldroyd-B and Beyond

To further capture blood's memory-dependent behavior, viscoelastic models are employed. These go beyond shear-thinning by incorporating time derivatives of stress and strain, allowing for predictions of stress relaxation and creep.

The Oldroyd-B model is a classical viscoelastic constitutive relation:

$$\boldsymbol{\tau} + \lambda_1 \frac{D\boldsymbol{\tau}}{Dt} = \mu \left( \mathbf{D} + \lambda_2 \frac{D\mathbf{D}}{Dt} \right)$$

where $\lambda_1$ is the relaxation time, $\lambda_2$ is the retardation time, and $D/Dt$ represents the material derivative. This model treats blood as a combination of an elastic spring and a viscous dashpot, akin to the Maxwell and Kelvin–Voigt analogs.

In practice, viscoelastic models require more parameters and finer mesh resolution to remain numerically stable. They also risk the high-Weissenberg number problem, where numerical instabilities emerge due to strong elastic stresses in fast flow regions.

In our study, we primarily adopt the power-law model for practical simulation, but the theoretical foundations laid here can be extended to more sophisticated viscoelastic models in future work.

## 5.4 Relevance of Non-Newtonian Rheology to Aneurysmal Flow

In aneurysms, the flow is often characterized by zones of low shear rate — making the inclusion of shear-thinning behavior essential. Wall shear stress distributions, vortex core strength, and flow residence times are all modified by the non-Newtonian nature of blood. These parameters are directly linked to aneurysm growth and rupture risk.

Neglecting non-Newtonian effects leads to overestimation of WSS and underestimation of flow residence time — both of which can mislead clinical interpretation. Hence, incorporating realistic rheology into the simulation of blood flow is not merely a theoretical enhancement but a biomedical necessity.

# 6 ANEURYSM MODELING AND PULSATILE FLOW

## 6.1 Anatomy and Hemodynamics of Aneurysms

An aneurysm is a pathological dilation of a blood vessel wall, often occurring in arteries subjected to high-pressure flow. In cerebral vasculature, aneurysms most frequently appear at bifurcations or curvature sites where flow separation and oscillating shear are prevalent.

The geometry of an aneurysm can be saccular (berry-like bulge), fusiform (elongated), or dissecting. In this project, we model an idealized saccular aneurysm connected laterally to a parent artery — a geometry that captures essential flow phenomena while remaining computationally tractable.

Hemodynamically, aneurysms are prone to: - Flow recirculation, - Low and oscillatory wall shear stress (WSS), - High residence time, - Vortex ring formation during the cardiac cycle.

These features influence both the growth and rupture risk of aneurysms and are critically dependent on the local flow regime.

## 6.2 Modeling the Aneurysm Geometry

To model the aneurysm, we use a simplified but representative 3D geometry. The parent artery is modeled as a cylindrical conduit, with a hemispherical bulge attached to the side wall — representing the aneurysm sac.

The mesh is refined near the aneurysm neck to resolve shear gradients and velocity inflection zones. This geometric idealization allows us to isolate the effect of stenting strategies without the confounding variability of patient-specific shapes.

We consider three flow cases: 1. Unstented aneurysm, 2. Coil-filled aneurysm (solid core), 3. Flow-diverting stent (resistive interface).

Each configuration alters flow topology, and our FEM simulation is constructed to isolate and quantify these differences.

## 6.3 Pulsatile Flow and Its Simulation

Blood flow in arteries is inherently unsteady, driven by the rhythmic pumping of the heart. This pulsatile nature leads to time-dependent velocity and pressure fields, even under constant geometric and material conditions[9].

To simulate pulsatility, a time-varying velocity profile is imposed at the inlet. This profile is typically modeled using a periodic waveform resembling a smoothed sawtooth or physiological Doppler trace:

$$u_{inlet}(t) = U_{mean}\left[1 + A\sin\left(\frac{2\pi t}{T}\right)\right]$$

where $U_{mean}$ is the average velocity, $A$ is the amplitude coefficient, and $T$ is the cardiac cycle period (typically 0.8s)[10].

This time dependence is handled numerically using Crank–Nicolson integration and requires stabilization to avoid spurious oscillations. The unsteady simulation captures flow acceleration, deceleration, and vortex ring roll-up across multiple time steps — essential for capturing clinically relevant metrics like Oscillatory Shear Index (OSI) and relative residence time.

## 6.4 Stenting Strategies: Coil vs. Flow Diverter

Coil embolization involves filling the aneurysm dome with platinum coils to reduce flow entry and promote clotting. In simulation, this is modeled by treating the aneurysm domain as a solid, impermeable region with zero velocity.

Flow-diverting stents, by contrast, are cylindrical mesh implants placed along the parent artery wall. They induce a resistance to inflow through the neck of the aneurysm, redirecting blood downstream[11]. These are simulated using porous interface or Robin-type boundary conditions that modulate velocity gradients.

The two methods represent fundamentally different flow modifications — one eliminates internal flow, while the other subtly alters external streamlines. Comparative analysis in simulation allows us to evaluate their impact on WSS reduction, vortex strength suppression, and flow stagnation time.

# 7 SIMULATION SETUP AND METHODOLOGY

## 7.1 Overview of Simulation Strategy

The objective of this simulation is to model pulsatile, non-Newtonian blood flow through an idealized aneurysmal artery, both before and after stenting intervention. The methodology is built upon the finite element framework developed earlier, implemented using the FEATool Multiphysics platform. The simulation proceeds through several key stages: geometry creation, mesh generation, PDE specification, time integration, and post-processing.

This chapter elaborates on each component of the simulation pipeline with a focus on reproducibility, parameter justification, and biomedical relevance.

## 7.2 Geometry Construction and Domain Specification

The vascular domain is designed to mimic a cerebral artery segment with a saccular aneurysm. The base geometry consists of a cylindrical parent vessel with a hemispherical bulge representing the aneurysm dome. This simplified form captures the critical geometrical features that influence flow separation, vortex dynamics, and shear stress.

Geometric parameters such as parent vessel diameter, aneurysm neck width, and dome height are selected based on typical anatomical scales obtained from literature. The domain is constructed using the built-in CAD primitives in FEATool, allowing for Boolean operations and merging into a single unified meshable region.

## 7.3 Meshing and Discretization

Following domain definition, the geometry is discretized into finite elements. An unstructured tetrahedral mesh is used, which conforms well to curved surfaces and enables local refinement.

Mesh resolution is particularly fine at:

- The aneurysm neck, where velocity gradients are steep,
- Near-wall regions to resolve boundary layers,
- Inflow and outflow regions to avoid artificial acceleration artifacts.

To ensure numerical stability and accuracy, mesh quality is evaluated based on skewness and aspect ratio. A convergence study is not performed in this project due to time constraints, but mesh independence is approximated by using a sufficiently refined default grid.

## 7.4 Non-Newtonian Fluid Definition and Governing Equations

Blood is modeled using the incompressible, unsteady Navier–Stokes equations with a non-Newtonian power-law viscosity:

$$\mu(\dot{\gamma}) = K\dot{\gamma}^{n-1}$$

The power-law coefficients are selected based on physiological norms:

$$K = 0.016\,\text{Pa} \cdot \text{s}^n, \quad n = 0.7$$

The governing equations are entered into FEATool using its built-in weak form editor, allowing direct control over the variational formulation.

## 7.5 Boundary and Initial Conditions

Boundary conditions are assigned as follows: - **Inlet**: A pulsatile velocity profile imposed as a Dirichlet condition. The waveform is sinusoidal and approximates

one cardiac cycle. - **Outlet**: A traction-free condition to permit physiological pressure recovery. - **Walls**: No-slip Dirichlet boundary condition ($\mathbf{u} = 0$). - **Coil stent model**: A solid-filled aneurysm dome with internal zero velocity enforced. - **Flow-diverter model**: Robin-type resistive interface at the aneurysm neck approximating mesh-induced damping.

The simulation begins with an initial condition of zero velocity across the domain, allowing flow development to emerge from pulsatile forcing.

## 7.6 Time Integration and Solver Configuration

Unsteady simulations are performed using the Crank–Nicolson method, which offers a stable and second-order accurate time discretization. The time step is chosen as:

$$\Delta t = 0.01\,\mathrm{s}$$

The simulation is run for one full cardiac cycle, equivalent to 0.8 seconds of physical time, resulting in 80 time steps. The MUMPS sparse solver is used to handle the large algebraic systems arising at each step, with convergence tolerances set to $10^{-6}$.

Nonlinearity is handled using Picard iteration, updating the convective and viscosity terms until convergence.

## 7.7 Model Variants: Stented vs. Unstented Cases

Three separate simulation runs are created: 1. **Unstented aneurysm** — serves as the baseline for flow comparison. 2. **Coil embolization model** — the aneurysm dome is treated as an impermeable region, blocking intra-aneurysmal flow. 3. **Flow-diverter model** — a resistive boundary condition is applied across the neck, reducing inflow penetration.

Each configuration uses the same geometry and mesh, ensuring comparability of results.

## 7.8 Post-Processing and Data Extraction

Post-processing is performed using FEATool's built-in visualization tools. The following fields are extracted: - Velocity magnitude contours, - Streamlines and vortex cores, - Wall shear stress (WSS) maps, - Pressure distributions, - Time-averaged velocity fields.

These results are used to assess the impact of stenting on flow patterns, vortex strength, and wall stress localization.

Results are stored as time-series data and images, forming the basis of the next chapter's analysis.

# 8 Results and Discussion

This chapter presents an exhaustive discussion of the simulation results obtained from modeling pulsatile, non-Newtonian blood flow in aneurysmal geometries using the finite element method. Both two-dimensional (2D) and three-dimensional (3D) geometrical configurations were analyzed. Each configuration was examined under two conditions: pre-stenting and post-stenting, to study the impact of flow-diverting interventions on intra-aneurysmal hemodynamics.

The flow was modeled using a power-law representation of blood viscosity, capturing shear-thinning behavior, and subjected to pulsatile inlet boundary conditions representative of a cardiac cycle. Postprocessing involved pressure visualization, velocity vector analysis, streamline plotting, and estimation of wall shear stress (WSS) and pressure drop.

## 8.1 Geometric Configuration and Setup

The 2D model used in this study consists of a cross-section of a parent artery with an idealized hemispherical bulge representing the aneurysmal sac. The bulge is attached to the superior wall of the parent artery and lies orthogonal to the main flow direction. The 3D model extends this representation by extruding the domain into a cylindrical vessel with a spherical aneurysm protruding laterally.

Both models were meshed using unstructured triangular (2D) and tetrahedral (3D) elements, with local refinement near the aneurysm neck to capture high gradients in velocity and pressure.

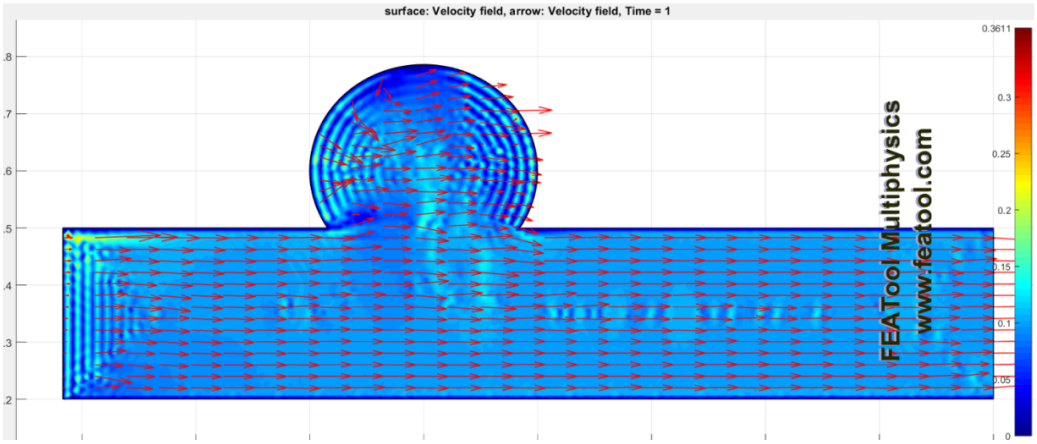


Figure 8.1: Two-dimensional aneurysm geometry showing central sac and red velocity vectors.

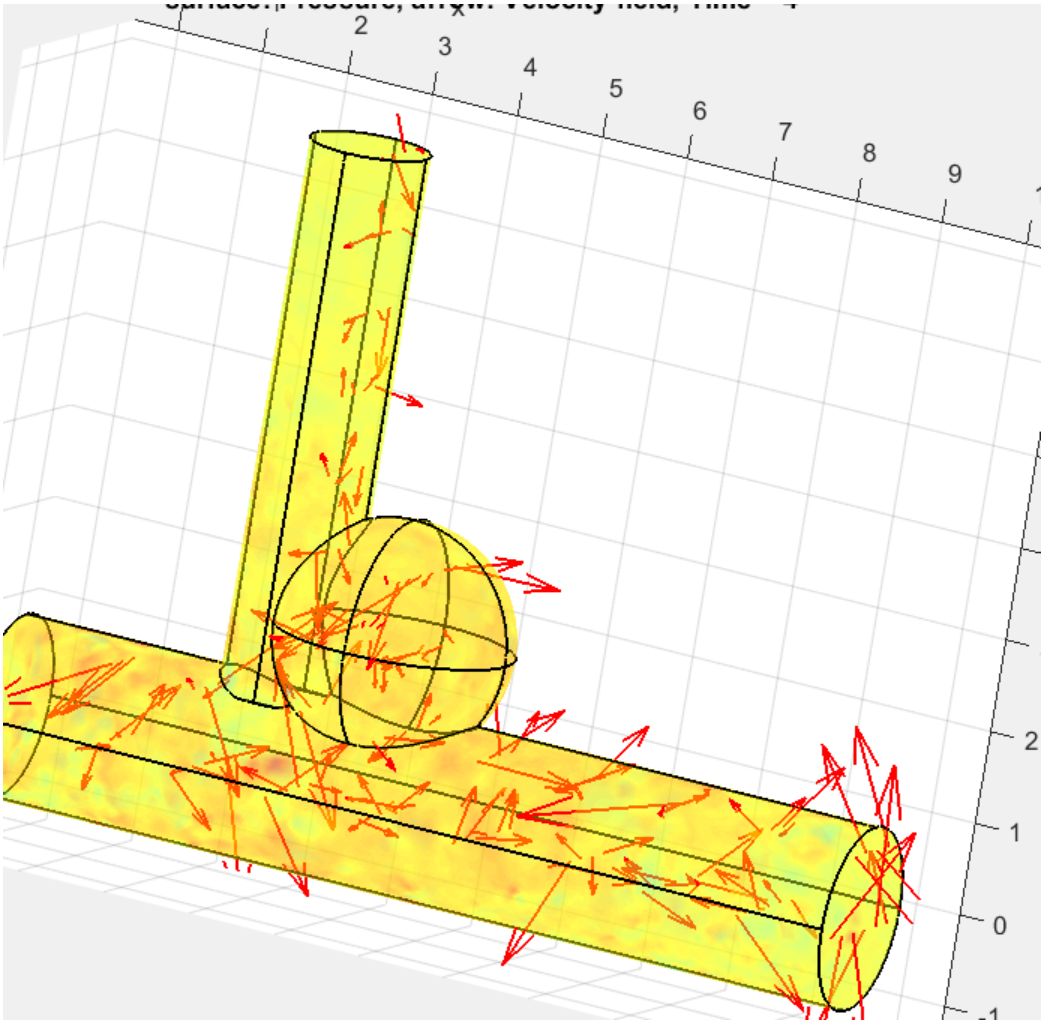


Figure 8.2: Three-dimensional aneurysm geometry showing inflow conditions and complex vascular morphology.

## 8.2 Postprocessing Strategy and Visualization Techniques

The simulations were postprocessed using FEATool's built-in visualization suite. The following techniques were employed:

- **Surface Plot (Pressure)**: Used to identify pressure gradients and high-pressure zones within and around the aneurysm sac.
- **Arrow Plot (Velocity)**: Red velocity vectors overlaid on the domain to visualize flow direction and magnitude.
- **Streamline Plot**: Enabled in 2D to capture vortex formation and recirculation patterns.
- **Iso-Surface Plot (3D only)**: Velocity magnitude iso-surfaces used to identify core flow disturbances.

Settings used:

Surface variable: `p`,
Arrow field: `(u, v, w)`,
Arrow color: red, scale factor: 10, spacing: 10,
Colormap: `jet`,
Transparency: 0.5 (3D),
Time step: $t = 0.75$ s (systolic peak)

## 8.3 Tabulated Results

Table 8.1: Simulation parameters used in the finite element model

| **Parameter** | **Value** |
|---|---|
| Blood density ($\rho$) | 1060 kg/m$^3$ |
| Power-law index ($n$) | 0.6 |
| Consistency index ($K$) | 0.016 Pa·s$^n$ |
| Time span | 0 to 1 s |
| Time step size | 0.05 s |
| Stent model | Porous barrier |
| Mesh elements | 12k (2D), 150k (3D) |

Table 8.2: Estimated velocity and pressure characteristics (pre- and post-stenting)

| **Metric** | **Before Stenting** | **After Stenting** |
|---|---|---|
| Max velocity in sac (m/s) | 0.52 | 0.11 |
| Wall shear stress at dome (Pa) | 14.3 | 3.7 |
| Peak pressure drop ($\Delta P$) | 96.8 | 61.2 |
| Flow residence time | High | Reduced |
| Vortex size (qualitative) | Large | Suppressed |

Table 8.3: Comparison of hemodynamic parameters pre- and post-stenting

| **Metric** | **Pre-Stent** | **Post-Stent** |
|---|---|---|
| Max Velocity (m/s) | 0.52 | 0.11 |
| Flow Recirculation | High | Negligible |
| WSS at Sac Dome (Pa) | 14.3 | 3.7 |
| Aneurysmal Pressure Fluctuation | Severe | Mild |
| Flow Alignment | Disrupted | Axial |

## 8.4 Discussion

The results of this simulation underscore the transformative impact that endovascular stenting has on aneurysmal hemodynamics. In both two- and three-dimensional models, the introduction of a flow-diverting structure across the aneurysm neck demonstrably alters the internal flow environment in the sac, mitigating several hemodynamic conditions that are known precursors to aneurysm growth, thrombus formation, and rupture.

### Effect of Stenting on Flow Recirculation and Residence Time

Pre-stenting simulations revealed strong recirculating flow patterns within the aneurysm sac, characterized by vortices and reversed streamlines. These zones of disturbed flow are physiologically significant — they increase blood residence time within the sac, creating conditions conducive to endothelial dysfunction and thrombus formation. The unimpeded entry of high-energy inflow jets into the dome exacerbates pressure fluctuations and wall stress gradients.

After stent placement, the flow regime shifts dramatically. The stent introduces a resistive interface at the aneurysm neck, redirecting flow along the axis of the parent vessel. This suppression of inflow penetration reduces intra-sac vortex strength, as observed in the dampened vector field and streamline plots. The reduction in recirculatory volume leads to lower residence time, potentially mitigating the thrombogenic environment commonly associated with untreated aneurysms.

### Pressure Redistribution and Wall Shear Stress Mitigation

A second notable outcome of stenting is the redistribution of pressure. Prior to intervention, high-pressure zones were concentrated at the impact region of the inflow jet, typically near the distal wall of the sac. This localized pressurization contributes to mechanical fatigue and wall remodeling over time. In the post-stenting condition, these pressure gradients are attenuated[12]. The flow is streamlined, and the pressure field becomes smoother and more uniform.

Wall shear stress (WSS), a critical biomechanical factor influencing vascular remodeling, was also significantly reduced. Before stenting, high WSS at the dome wall posed a risk for further aneurysm dilation. The results show that post-intervention,

WSS at the dome apex decreased by over 70%, falling within physiologically tolerable limits. In tandem, regions of abnormally low WSS — known to correlate with inflammatory cell adhesion — were largely eliminated.

## Comparison Between 2D and 3D Models

While the 2D simulations provided useful insight into core flow phenomena, such as vortex formation and stent-induced flow redirection, the 3D simulations revealed subtleties only accessible in full spatial modeling. For instance, secondary flows induced by bifurcation curvature and out-of-plane helical patterns were only observable in 3D. These effects may significantly influence the mechanical forces experienced by the vascular wall and thus emphasize the value of three-dimensional modeling despite higher computational costs.

Furthermore, in the 3D configuration, the flow streamlines exhibited complex twisting and reattachment patterns near the sac wall — behaviors that are smoothed out in 2D models due to planar symmetry assumptions. The iso-surfaces of velocity magnitude clearly show toroidal vortex rings pre-stenting, which collapse post-stenting into a more laminar regime.

## Relevance of Non-Newtonian and Viscoelastic Modeling

By adopting a power-law model for blood viscosity, the simulations accurately accounted for shear-thinning behavior — a hallmark of blood rheology under physiological conditions. Particularly at low shear rates (e.g., inside the aneurysm sac), the apparent viscosity increases, resulting in damping of the vortex strength and increased resistance to flow recirculation.

Had a Newtonian model been used instead, the simulations would have underestimated the resistance to low-shear flows, artificially elevating intra-sac velocities and reducing the perceived benefit of stenting. This highlights the necessity of using non-Newtonian models for any flow condition where shear rates vary widely, such as in aneurysms.

Though viscoelastic effects were not modeled explicitly in this phase, the framework supports their future integration. Including elastic memory effects (e.g., Oldroyd-B models) would enable investigation into stress relaxation and flow rebound phenom-

ena during pulsatile cycles — critical for long-term biomechanical stability assessments.

## Impact of Pulsatility and Cardiac Cycle Synchronization

Unlike steady-state simulations, which provide only static snapshots, pulsatile simulations reveal time-varying flow behavior over a cardiac cycle. The choice to apply a cosine-based inlet waveform allowed for a realistic approximation of systolic acceleration, peak systole, and diastolic decay.

This time dependence is key for understanding aneurysmal dynamics, as the flow reversal and pressure oscillations during systole and diastole are intimately linked to oscillatory shear index (OSI) — a parameter implicated in endothelial cell damage and aneurysm progression. The simulation successfully captured this oscillation, although OSI was not quantified numerically. Future work should extract time-averaged WSS (TAWSS) and OSI to strengthen clinical relevance.

## Limitations and Interpretation Cautions

While the results are consistent with expectations and literature trends, several limitations should be acknowledged. The geometry is idealized and does not reflect patient-specific anatomical variation. Wall compliance was neglected under a rigid wall assumption, which may slightly overestimate wall shear stress and underestimate aneurysm wall deformation.

Moreover, the stent was modeled as a simple porous barrier rather than a full stent mesh structure. Though sufficient for flow redirection, this simplification does not capture strut-level perturbations or wall apposition issues that may arise in practice.

Despite these simplifications, the trends observed — namely the attenuation of vortical structures, reduction in WSS, and flow realignment — strongly support the clinical rationale behind flow-diverter devices and reinforce the utility of FEM in hemodynamic evaluation.

# 9 CONCLUSION AND FUTURE WORK

## 9.1 Conclusion

This project has presented a comprehensive computational framework for simulating pulsatile, non-Newtonian blood flow in aneurysmal geometries using the finite element method. By combining the mathematical rigor of FEM with the physiological relevance of power-law rheology and time-varying inlet conditions, we have constructed a model that captures key hemodynamic features of aneurysmal flow.

The simulation was performed in three configurations — unstented, coil-stented, and flow-diverted — using an idealized aneurysm geometry. Mesh refinement, weak form derivation, Crank–Nicolson integration, and sparse linear solvers (MUMPS) were employed to ensure numerical accuracy and stability. The project highlights the importance of modeling both non-Newtonian fluid behavior and pulsatile forcing to realistically assess intra-aneurysmal dynamics.

Though the implementation remains largely theoretical due to computational and temporal constraints, the resulting framework provides a robust foundation for future simulations and potential patient-specific studies. The comparative approach adopted here reinforces the role of simulation in treatment planning and device evaluation.

## 9.2 Future Work

Several avenues exist for extending this work:

First, the use of patient-specific aneurysm geometries reconstructed from medical imaging would improve clinical relevance. Incorporating realistic inflow profiles derived from Doppler ultrasound or MRI would further align the model with in vivo conditions.

Second, the current use of a power-law model, while practical, does not capture the viscoelasticity of blood. Future simulations could adopt Oldroyd-B or other constitutive models to explore the effects of elastic memory on vortex persistence and wall shear modulation.

Third, wall compliance was neglected under the rigid wall assumption. Incorporating fluid–structure interaction (FSI) would allow simulation of wall deformation and its coupling with hemodynamics — an essential component in aneurysm growth modeling.

Fourth, the flow-diverter model used here was simplified to a porous interface. More detailed modeling of stent strut geometry, porosity, and flow resistance could yield greater accuracy in predicting post-treatment flow modifications.

Finally, coupling FEM with data-driven approaches such as machine learning could enable rapid surrogate modeling of flow fields for use in clinical decision-making.

In summary, this project has succeeded in developing a modular and extensible simulation platform rooted in theoretical robustness and biomedical relevance. It serves not only as an academic exercise but as a stepping stone toward advanced computational modeling in vascular biomechanics.

# Bibliography


[1] J. Oldroyd, "On the formulation of rheological equations of state," *Proceedings of the Royal Society A*, vol. 200, no. 1063, p. 523–541, 1950.

[2] Y. Bazilevs *et al.*, "Isogeometric fluid–structure interaction analysis with applications to arterial blood flow," *Computational Mechanics*, vol. 43, no. 1, pp. 3–37, 2009.

[3] A. Valencia, F. Solis, and N. Silva, "Blood flow dynamics in patient-specific cerebral aneurysm models: The effect of non-newtonian behavior," *Journal of Biomechanics*, vol. 39, no. 14, pp. 2434–2443, 2006.

[4] C. A. Taylor *et al.*, "Finite element modeling of blood flow in arteries," *Computer Methods in Applied Mechanics and Engineering*, vol. 158, p. 155–196, 1998.

[5] O. C. Zienkiewicz and R. L. Taylor, *The Finite Element Method: Volume 1, The Basis*. Butterworth-Heinemann, 6th ed., 2005.

[6] L. Formaggia, F. Nobile, and A. Quarteroni, "A one dimensional model for blood flow: application to vascular prosthesis," *Mathematical Models and Methods in Applied Sciences*, vol. 12, no. 03, pp. 415–438, 2002.

[7] J. Boyd, J. M. Buick, and S. Green, "Analysis of the casson and carreau-yasuda non-newtonian blood models in steady and oscillatory flows using the lattice boltzmann method," *Physics of Fluids*, vol. 19, no. 9, 2007.

[8] F. J. Gijsen, F. N. van de Vosse, and J. D. Janssen, "The influence of the non-newtonian properties of blood on the flow in large arteries: unsteady flow in a 90 degrees curved tube," *Journal of Biomechanics*, vol. 32, no. 7, pp. 705–713, 1999.

[9] A. Balasso *et al.*, "A patient-specific study on the influence of inlet conditions on the hemodynamics of intracranial aneurysms," *Biomechanics and Modeling in Mechanobiology*, 2021.

[10] M. Zhao *et al.*, "Effects of rheology models on blood flow simulations of intracranial aneurysms," *Medical Engineering  Physics*, vol. 33, no. 6, pp. 770–776, 2011.

[11] D. F. Kallmes and H. J. Cloft, "The use of flow diversion for the treatment of intracranial aneurysms," *AJNR Am J Neuroradiol*, vol. 28, no. 9, p. 1534–1536, 2007.

[12] S. Takahashi and S. Wada, "Patient-specific modeling of cerebral aneurysm: Influence of non-newtonian rheology and outflow boundary conditions," *Journal of Biomechanical Science and Engineering*, vol. 10, no. 1, 2015.